Published in final edited form as:
Virology. 2010 May 25; 401(1): 49–60. doi:10.1016/j.virol.2010.01.020.

VACCINIA H5 IS A MULTIFUNCTIONAL PROTEIN INVOLVED IN VIRAL DNA REPLICATION, POSTREPLICATIVE GENE TRANSCRIPTION, AND VIRION MORPHOGENESIS

Susan M. D'Costa[1,*], **Travis W. Bainbridge**[1,3], **Sayuri E. Kato**[1], **Cindy Prins**[1,4], **Karen Kelley**[2], and **Richard C. Condit**[1]

[1]Department of Molecular Genetics and Microbiology, University of Florida, Gainesville, FL, 32610-0266

[2]Interdisciplinary Center for Biotechnology Research (ICBR) Electron Microscopy And Bio-Imaging Laboratory, University of Florida, Gainesville, FL, 32610-0266

Abstract

The vaccinia H5 protein has been implicated in several steps of virus replication including DNA synthesis, postreplicative gene transcription, and virion morphogenesis. Our recent mapping of mutants in the consolidated Condit-Dales collection identified a temperature-sensitive vaccinia mutant in the H5R gene (Dts57). We demonstrate here that Dts57 has a DNA negative phenotype, strongly suggesting a direct role for H5 in DNA replication. We used a temperature shift protocol to determine the impact of H5 temperature sensitivity on postreplicative gene expression and observed changes in the pattern of postreplicative viral mRNA metabolism consistent with a role of H5 in postreplicative transcription. Finally, using a rifampicin-release temperature-shift protocol, we show that H5 is involved in multiple steps of virion morphogenesis. These data demonstrate directly that H5 plays roles in DNA replication, transcription and morphogenesis *in vivo*.

Keywords

poxvirus; vaccinia; ts; H5; DNA replication; postreplicative gene transcription; virion morphogenesis; scaffold

Introduction

Poxviruses are large (~200 kb) double-stranded DNA viruses that replicate exclusively in the cytoplasm of the infected cell and encode their own nucleic acid metabolism machinery (Moss, 2007). The prototypical and therefore the best studied member of this family is vaccinia virus. Viral gene expression during vaccinia infection occurs in a temporal cascade that is regulated by several viral and host factors. Of the three classes of genes, early gene expression precedes

*Address correspondence to: Susan M. D'Costa, Ph.D, PO Box 100266, JHMHC, University of Florida, Gainesville, FL 32610. Phone: 352-273-7513; Fax: 352-273-8905; ihssd@ufl.edu .
[3]Current Address: Department of Protein Chemistry, Genentech, Inc., 1 DNA Way, South San Francisco, CA 94080
[4]Department of Infection Prevention and Control, Shands Hospital at the University of Florida, Box 100153 Gainesville, FL 32610

viral DNA replication whereas intermediate and late (collectively termed postreplicative) gene transcription is coupled to and therefore occurs concomitantly with DNA replication. Early gene products are required for DNA replication and many of the postreplicative proteins are involved in virion morphogenesis. Notwithstanding this temporal regulation of gene expression, several viral proteins are expressed throughout the virus life cycle. Viral DNA replication, postreplicative transcription and virion assembly take place in discrete cytoplasmic sites termed virus factories. Virion assembly commences with formation of crescent shaped viral membrane structures within factories, followed by packaging of condensed viroplasm and DNA within the viral membranes to form spherical immature virions with nucleoids (IVN), and completed with proteolysis of major virion structural proteins and metamorphosis of the IVN into mature virions (MV) accompanied by transport of the MV out of the factory.

The vaccinia H5R gene has been implicated in virtually all phases of the virus life cycle, including DNA synthesis, postreplicative gene transcription, and virion morphogenesis. The H5R gene is highly conserved in the chordopoxviruses but is absent from the entomopoxviruses. H5 is a 22.3 kDa phosphoprotein that is constitutively expressed in abundance during viral replication, localized in viral factories and packaged into virions (Rosel et al., 1986). H5 is phosphorylated by both viral kinases (F10 and B1) and cellular kinases but the pattern of phosphorylation is dynamic and temporally regulated (Beaud et al., 1995; Condit et al., 2006). Additionally, H5 is a nucleic acid binding protein with affinity for both DNA and RNA (Kay, N., Bainbridge, T, Condit, C. and D'Costa, S., unpublished results; (Beaud et al., 1995; Kovacs & Moss, 1996; Nowakowski et al., 1978). H5 has been shown to stimulate late transcription *in vitro* and it interacts with viral late transcription initiation (A2 and G8), elongation (G2) and termination (A18) factors, suggesting a role for H5 in postreplicative transcription (Kovacs & Moss, 1996; Dellis et al., 2004; McCraith et al., 2000; Black et al., 1998). Importantly, an H5 mutant has been isolated which is resistant to isatin beta-thiosemicarbazone (IBT), an antipoxvirus drug that is known to affect vaccinia postreplicative gene elongation (Cresawn & Condit, 2007), thus substantiating a role for H5 in postreplicative gene transcription. Additionally, biochemical analysis demonstrates that H5 is associated with endoribonuclease activity that processes at least two vaccinia late mRNAs, suggesting a role for H5 in late transcription termination (D'Costa et al., 2008). H5 also interacts with A20, the viral DNA replication processivity factor, and B1, a viral protein kinase required for viral DNA replication (Ishii & Moss, 2001; McCraith et al., 2000), implying a role for H5 in DNA replication. In order to confirm a role for H5 in DNA replication, DeMasi and coworkers engineered a ts mutant in H5R, tsH5–4, using clustered-charge to alanine scanning mutagenesis (Demasi & Traktman, 2000). Surprisingly, this mutant was not defective in DNA replication but instead was shown to have a defect in early morphogenesis, adding yet another role for H5 in virus replication.

Recently, our laboratory identified in the consolidated Condit-Dales collection a temperature-sensitive vaccinia mutant (Dts57) that maps to the H5R gene (Lackner et al., 2003; Kato et al., 2008). In this study, we show that Dts57 has a DNA negative phenotype, confirming a central role for H5 in DNA replication. Using a temparature shift protocol we show that postreplicative transcription is adversely affected in Dts57 infections. Finally, using a rifampicin release, temperature shift protocol, we show that functional H5 is required both for inclusion of virosoplasm into crescents as well as for maturation of IVs into MVs.

Results

Marker rescue and DNA sequencing

The temperature-sensitive mutant, Dts57, has been placed in a complementation group by itself (Lackner et al., 2003). In order to determine the gene to which it mapped, four rounds of marker rescue were carried out (Kato et al., 2008). Confluent monolayers of BSC40 cells were infected

with Dts57 and transfected with DNA fragments PCR-amplified from wild type vaccinia virus genomic DNA. The first round of marker rescue used pools of overlapping 20 kb fragments spanning the entire vaccinia virus genome (not shown), the second round resolved the map position to a single 20 kb fragment (not shown), the third round used overlapping 5 kb PCR products spanning the 20 kb region of the vaccinia genome that scored positive in round two and the last round resolved the map to a single gene contained within the 5 kb fragment that scored positive in round three (Fig. 1) (Kato et al., 2008; Luttge & Moyer, 2005; Yao & Evans, 2003). Marker rescue of Dts57 with individual ORFs in the 5-kb LM22 region indicated a rescue with the H5R gene (Fig. 1D). However, this signal was only weakly positive over background. Assuming that the mutation was close to the 5' or 3' end of the H5R gene, this rescue was repeated with overlapping PCR products spanning two adjacent ORFs within the D1R–H7R region. A successful rescue was obtained with both the H4R–H5R and the H5R–H6R products with a stronger signal over background in the latter rescue, suggesting that the mutation was near the 3'end of the H5R gene.

The H5R gene from Dts57, WR, and IHDW was sequenced as described in Materials and Methods. The H5R gene from IHDW was sequenced because it is the parent strain from which Dts57 was derived (Dales et al., 1978). In addition, the H5R gene from WR was sequenced to determine potential polymorphisms between these two wild-type strains routinely used in our laboratory. No polymorphisms were detected between the parental IHDW and WR strains (data not shown). In contrast there was one non-coding polymorphism in the H5R gene of these viruses compared to the published WR sequence. (The published WR sequence is from a different WR isolate than the WR isolate used in our laboratory (Condit & Motyczka, 1981)). Finally, Dts57 contained a single point mutation at nucleotide 566, resulting in an amino acid substitution from glycine to arginine at position 189 (G189R). The sequencing data are in good accordance with the marker rescue data and confirmed that the mutation was indeed near the 3' end of the 203 codon H5R gene.

Growth properties of Dts57

The temperature-sensitivity of Dts57 was ascertained by carrying out a one-step growth experiment. BSC-40 cell monolayers were infected with either wt IHDW or Dts57 virus at an moi of 10 at both 31°C and 39.7°C. At different times post-infection, cells and media were harvested and the virus yield at each time was determined by a plaque assay performed at 31° C (Fig. 2). IHDW grew normally at both 31°C and 39.7°C. Dts57 grew well at 31°C but nevertheless grew slightly slower and reached slightly reduced titers compared to IHDW grown at 31°C. Dts57 grown at 39.7°C did not yield any infectious progeny confirming the temperature sensitivity of this mutant.

Basic phenotypic characterization of Dts57

Our preliminary analysis indicated that Dts57 was defective in DNA synthesis (see Fig. 5). This was a novel finding given that a previously engineered ts mutant in H5R had a morphogenesis phenotype (Demasi & Traktman, 2000). In order to confirm our findings and also compare these data with a known DNA negative mutant, all further phenotypic characterizations of Dts57 were done in tandem with a wild-type IHDW control and Dts20, a DNA negative mutant in the vaccinia DNA polymerase gene (E9R). Studies with both DNA replication inhibitors and with DNA replication mutants have demonstrated previously that late viral gene expression is coupled to viral DNA replication, that is, when viral DNA replication is is prevented, postreplicative viral gene expression is inhibited and, presumably as a consequence, early viral gene expression is not shut off (Moss, 2007;Condit & Niles, 2002). Interestingly, McDonald et al (1992) have shown using metabolic inhibitors and temperature sensitive mutants that the gene expression patterns of at least some (DNA polymerase, D5, and B1 kinase) early genes are transient and unlinked to viral DNA replication

and late gene expression. For the most part however, viral gene expression as measured by protein and RNA synthesis can be used to corroborate a DNA negative phenotype. Therefore, we assayed viral protein and RNA synthesis as a measure of overall gene expression in mutant infections. Monolayers of BSC40 cells were infected with either Dts57, IHDW, or Dts20 at an moi of 10 and incubated at either 31°C or 39.7°C for analysis of both protein and mRNA synthesis (Fig. 3 and Fig. 4). In order to analyze protein synthesis, at various times post infection, infected cells were pulse labeled for 30 min in media containing ^{35}S-methionine and harvested in SDS-sample buffer. These samples were then fractionated on SDS-PAGE gels and analyzed by autoradiography. The time course of infection for Dts57 and Dts20 at 31°C was indistinguishable from IHDW at both 31°C and 39.7°C, showing in each case a shutoff of host proteins and a temporal cascade of early, intermediate, and late protein expression (Fig. 3). At the non-permissive temperature, the protein expression patterns for both Dts57 and Dts20 were similar to each other and significantly different than permissive infections, showing a decrease in host protein shutoff, extended synthesis of early proteins, and a lack of late protein expression consistent with a DNA negative phenotype. However, unlike Dts57, early protein expression appears to decay in Dts20 infections at late times post infection. This phenotype has been observed earlier for other DNA polymerase mutants (Sridhar & Condit, 1983) but not for other DNA negative mutants.

For the analysis of mRNA synthesis, BSC40 cells infected with Dts57, Dts20, or IHDW were harvested at various times post infection and RNA was extracted. RNA samples were fractionated on formaldehyde-agarose gels, the fractionated RNA was transferred to nylon membranes and the membranes were hybridized with ^{32}P-labeled riboprobes specific for either an early gene (C11R), an intermediate gene (G8R), or a late gene (F17R) (Fig. 4). For the wt infections (IHDW) at both temperatures, the early transcripts (C11R) peaked intially at 3 h p.i. followed by a second peak in synthesis later in infection either at 12 h p.i. (31°C) or at 9 h p.i. (39.7°C). This reactivation of early transcription has been previously observed for IHDW but not WR (Shatzer et al., 2008). At the permissive temperature, both Dts57 and Dts20 showed an initial peak of C11R transcripts at 3 h p.i. with a delay in the second peak of synthesis (15 h p.i.). Interestingly, at the non-permissive temperature, while C11R transcripts in the Dts57 infection peaked at 3 h p.i. and remained high for the remainder of the analysis, in Dts20 infections C11R transcripts decreased in amount to near background levels after the initial peak at 3 h p.i., consistent with the pattern of protein synthesis observed in Fig. 3. Thus Dts57 infections display the extended synthesis of early gene products typical of most inhibitors of DNA replication while Dts20 infections display the decay of early gene expression apparently unique to DNA polymerase mutants (Sridhar & Condit, 1983). For the intermediate gene, G8, a peak of RNA synthesis was observed at 6 h p.i. (or 3 h p.i. at 39.7°C) for IHDW infections. In Dts57 and Dts20 infections, while the pattern of G8 transcription is similar to wt at the permissive temperature, there is merely a background level of transcription at the non-permissive temperature, confirming again the DNA negative phenotype of these mutants. Finally, for the late gene, a peak of F17 transcripts is observed at 9 h p.i (6 h p.i. at 39.7°C) in IHDW infections. On the other hand in both Dts57 and Dts20 infections, there is a delay in synthesis of F17 transcripts as compared with wt (12 h p.i.) at the permissive temperatures and no synthesis at the non-permissive temperature, consistent with a block in DNA replication.

H5 influences late transcription

Since H5 has been implicated in multiple steps of vaccinia virus replication including postreplicative transcription and viral morphogenesis, we were interested in analyzing events downstream of DNA replication in a Dts57 mutant infection. Because the late phase of infection is inhibited in the absence of DNA replication, we employed a temperature shift protocol to examine the effects of H5 temperature sensitivity on postreplicative gene expression. Cells were infected with either Dts57, IHDW, or Dts20 at both permissive and non-permissive

temperatures. A subset of the cells incubated at the permissive temperature was then shifted up to the non-permissive temperature at 9 h p.i. once DNA replication and late gene expression were well underway (Fig. 5). Samples were harvested at the various times indicated in Fig. 5 and analyzed for viral DNA, protein, and mRNA synthesis, virus yield, and H5 protein stability. Viral DNA synthesis was analyzed by slot blot hybridization of DNA in infected cell lysates to a radiolabeled vaccinia genome specific probe. Wild type viral DNA replication proceeded normally in infections maintained at 31°C and 39.7°C or in infections shifted from 31°C to 39.7°C. Mutant infections demonstrated normal DNA synthesis at 31°C and no DNA synthesis in infections maintained at 39.7°C from the beginning of infection. DNA replication was abrogated upon shift up of Dts57 and Dts20 infections from the permissive to the non-permissive temperature, thus both mutants possess a DNA negative phenotype (Fig. 5A). Despite the interruption in DNA replication, protein pulse labelling indicated that normal levels of late proteins were synthesized in both Dts57 and Dts20 infections post shift-up (Fig. 5B). Immunoblot analysis showed that the the steady state level of mutant H5 synthesized in Dts57 infections did not change when compared with the control infections indicating that the mutant H5 protein is not destabilized by the temperature shift (Fig. 5C). Analysis of virus yield (Fig. 5D) under conditions permissive for virus growth, that is 31°C for Dts57 and Dts20 and 31° C, 39.7°C or shift up from 31°C to 39.5°C for IHDW, showed a 10–80 fold increase in virus titer at 24 hr compared to 0 hr, as expected. Mutant infections maintained at 39.7°C showed no increase in titer at 24 hr, also as expected. Shifting Dts20 infections from 31°C to 39.7°C resulted in a a 6-fold increase in titer within 24 h, suggesting a partial inhibition of virus growth. However in Dts57 infections there was no increase in titer between 0 and 24 hr in infections shifted from 31°C to 39.7°C. This suggests that H5 may be involved in events downstream of DNA replication.

In order to analyze the role of H5 in mRNA synthesis, RNA was harvested during the shift up experiment as described above, and northern blots were prepared and hybridized to riboprobes specific for three genes representative of each temporal class, early (C11R), intermediate (G8R) and late (F17R) (Fig. 6). Importantly, previous experiments demonstrating a coupling of viral DNA replication and postreplicative gene transcription have used protocols which block DNA replication from the outset of infection. Therefore, in addition to assessing the effect of H5 temperature sensitivity on postreplicative gene transcription, the temperature shift experiment done with a Dts20 control measures for the first time the impact on postreplicative transcription of interrupting ongoing viral DNA replication. For the C11R early gene, in both IHDW and Dts20 infections, shift up to the non-permissive temperature caused an increase in signal intensity at 12 h p.i. However, in the Dts57 infection, a shift up to the non-permissive temperature resulted in a decrease in signal intensity for the C11R transcript. These results are contrary to expectations based on infections with Dts20 and Dts57 maintained at 39.7°C from the beginning of the infection (Fig. 4), where C11R transcription decayed in Dts20 infections but not in Dts57 infections. One possible explanation for this observation is that reactivation of early transcripts, a key feature of viruses in the IHDW strain lineage, is defective in Dts57 infections. In the case of the intermediate G8R gene transcripts, an increase in signal followed by a plateau is observed upon temperature shift in IHDW infections. Conversely, in both Dts57 and Dts20 infections, there is a decrease in intensity of the G8 transcript suggesting a decay of intermediate transcripts. The decay of the G8R appears more dramatic and immediate in Dts57 infections as compared with Dts20 infections, suggesting that H5 may be directly involved in intermediate transcription. Finally, for the late, F17R gene transcripts, a homogenous F17R transcript is observed in IHDW infections. The homogeneity of F17R transcript is as a result of a post-transcriptional endoribonucleolytic event (D'Costa et al., 2004). H5 has been identified to be associated with the endoribonuclease tactivity that catalyzes this cleavage event *in vitro* (D'Costa et al., 2008). The intensity of the F17R transcript remains constant upon shift up and until the end of the time course in IHDW infections. Interestingly, in both Dts57 and Dts20 infections, this homogenous band decreases in intensity upon shift up. However, an

interesting difference noted was the presence of a second, fairly homogenous, faster migrating band in Dts57 but not in Dts20 infections, suggesting that shorter than normal transcripts are produced in Dts57 infections,. Importantly, the decrease in post-replicative transcription in the absence of DNA synthesis does not appear to correlate with the apparently normal protein synthesis pattern (Fig. 5B) observed for both Dts20 and Dts57 infections under the same conditions. Shatzer et al (2008) observed a similar anomaly for capping enzyme (D1) mutant infections. Specific early genes were observed to be significantly decreased in expression even though a normal pattern of early protein synthesis was observed by protein pulse labeling. Thus metabolic labeling is not necessarily a reliable quantitative measure of mRNA metabolism. In summary, while subtle, the northern blots show that the phenotype observed for Dts57 infections is different from that seen for a classic DNA negative mutant and therefore suggest that H5 may play a direct role in vaccinia late transcription.

H5 is directly involved in virion morphogenesis

Previous phenotypic characterization of an engineered temperature sensitive mutant in H5R, tsH5–4, revealed a defect early in virion morphogenesis characterized by the establishment of factories devoid of any normal virion precursors and the formation of malformed or "curdled" virosomes (Demasi & Traktman, 2000). Because H5 is also implicated in postreplicative transcription (D'Costa et al., 2008; Kovacs & Moss, 1996; Dellis et al., 2004; Ishii & Moss, 2001; Cresawn & Condit, 2007; Ishii & Moss, 2002), the possibility exists that the phenotype observed for tsH5–4 is a pleiotrophic effect resulting from a subtle defect in late transcription. In our temperature shift protocol, we observed a decrease in virus production in Dts57 infections compared to Dts20 infections that could be attributed either to a subtle defect in transcription or to a defect in morphogenesis (Fig. 5). Therefore, we were motivated to explore further a possible role for H5 in virion morphogenesis. We employed a rifampicin release, temperature shift protocol that has been used previously to elucidate the functions of several vaccinia proteins including A13, F10, and G7 (Mercer & Traktman, 2005; Unger & Traktman, 2004; Punjabi & Traktman, 2005). Rifampicin does not affect vaccinia viral gene expression but specifically arrests vaccinia virus morphogenesis by preventing formation of a viral D13 protein-containing scaffold on which viral membrane crescents are formed (Szajner et al., 2005). Rifampicin treated cells accumulate large virosomes that are surrounded with loose or flaccid membranes, together called rif bodies. Upon removal of rifampicin morphogenesis resumes within minutes. Therefore, rifamicin can be used to synchronize infections at a point where postreplicative gene expression is effectively complete but morphogenesis is just beginning. BSC40 monolayers were infected with either IHDW, Dts57, or tsH5–4 virus (moi = 10) at 31°C in the presence of the drug rifampicin (Fig. 7). At 12 h p.i., cells were either harvested immediately or refed with media with and without rifampicin and incubated at the permissive temperature or shifted up to the non-permissive temperature for a further 24 h (36 h p.i.). At this time, the cells were processed either for determination of virus yield or for electron microscopy (Fig. 7A, Fig. 8). We chose 36 h p.i. as the time of harvest because Dts57 cultures maintained at 31°C after RIF release (positive control) needed a longer time to recover from the RIF block. Since the rifampicin sensitive step precedes proteolytic processing of virion proteins, we also analyzed proteolytic processing using a pulse-chase protocol and immunoblot analyses (Fig. 7B, C). For pulse-chase analysis, cells were infected at the permissive temperature in media containing rifampicin as described above. At 12 h p.i., the media was removed and the cells were labeled with ^{35}S-methionine in media containing rifampicin for 30 min. at 31°C. These pulsed cells were then either harvested immediately or refed with and without rifampicin and incubated at the permissive temperature or shifted up to the non-permissive temperature for a further 24 h (36 h p.i.), and then harvested for analysis by SDS-PAGE and autoradiography or immunoblot analysis, using A10 and G7 antibodies.

All three infections (wt IHDW and H5 mutants Dts57 and tsH5–4) maintained in the presence of rifampicin throughout infection showed background levels of virus yield (Fig. 7A, R31 and RS). In addition proteolytic processing of virion proteins was blocked (Fig. 7B and C) and rifampicin bodies accumulated (Fig. 8). When maintained at 31°C without rifampicin from 12 to 36 h p.i., all three infections recovered from the rifampicin block yielding a 100–1000 fold increase in titer (5–50 pfu/cell) (Fig. 7A, RR/31). Additionally, these infections showed normal processing of key virion proteins including p4a, and preG7 as determined by both pulse chase and immunoblot analyses (Fig. 7 B and C). Finally, all the normal stages of morphogenesis with virosomes (v), crescents (cr), immature virions (IV) and a large number of mature virions (MV) were observed by electron microscopy (data not shown). In contrast, Dts57 infections that were released from the rifampicin block and shifted up to 39.7°C showed no increase in titer (Fig. 7A, RR/S), and no proteolytic processing of key virion proteins (Fig. 7 B and C). Electron microscopy revealed that morphogenesis was arrested at the stage of IV formation (Fig. 8). We observed several examples of crescents "biting" off virosomes as well as several examples of normal looking IV, and some partially filled or dense IV. However, very few IVN and no MV were observed, suggesting that H5 is required for the maturation of immature to mature virions. By contrast, under conditions of rifampicin release and shift tsH5–4 appeared to have a partial arrest phenotype with a 20-fold (1 pfu/cell) increase in titer (Fig. 7A, RR/S). Pulse chase analysis showed a defect in proteolytic processing and immunoblot analysis showed that neither p4a nor preG7 were processed under these conditions (Fig. 7B and C). Additionally, preG7 protein appears to be unstable in tsH5–4 but not in Dts57 infections under these conditions, consistent with previous results for this mutant (Mercer & Traktman, 2005). After rifampicin release and shift, the cytoplasm of tsH5–4 infected cells showed large areas of clearing with several crescents, empty IV and a few dense IV by electron microscopy (Fig. 8). Additionally, we observed several examples of "curdled" virosomes (CV), a phenotype reminescent of tsH5–4 infections maintained at the non-permissive temperature from the outset of infection (Demasi & Traktman, 2000). The tsH5–4 phenotype under rifampicin release, temperature shift conditions is also very similar to that observed for tsG7 under the same conditions (Mercer & Traktman, 2005). Thus, while both Dts57 and tsH5–4 appear to be arrested at the stage of IV formation, the phenotype is different, suggesting multiple points of execution during morphogenesis.

Discussion

Using a temperature-sensitive mutant of H5R, Dts57, we have established that H5 is involved in multiple aspects of virus replication *in vivo*. Specifically, we have shown that Dts57 is a DNA negative mutant demonstrating that H5 is directly involved in DNA replication. We have also demonstrated using a temperature shift protocol that H5 influences postreplicative gene transcription. Finally using a rifampicin release, temperature shift protocol, we have determined that H5 is required for at least two separate steps in virion morphogenesis. We have adopted a scaffold model (Condit et al., 2006; Mercer & Traktman, 2005) to explain the varied roles of H5 in a unified structural context, described below.

The scaffold model for H5 function is founded on the observation that H5 is an abundant protein that apparently self associates to form a large complex. Using both yeast two hybrid analysis and co-immunoprecipitation, Dellis et al (2004) showed that H5 interacts with itself. We have shown previously that purified H5 (expressed either from vaccinia virus or as a recombinant protein in E. coli) elutes with a large molecular mass (~400 kDa) on a gel filtration column (D'Costa et al., 2008). Analysis in silico predicts that the N-terminus of the H5 protein is highly disordered (D'Costa and Condit, unpublished observations). Disorder in protein structure is thought to facilitate interaction via induced fit with multiple binding partners (Romero et al., 2004). Thus we predict that H5 multmerizes via its C terminus to form a scaffold and mediates its activities through interaction with multiple binding partners through its N terminus. The

interaction of H5 with numerous proteins involved in DNA replication, transcription and assembly is well known as detailed below. H5 is also a nucleic acid binding protein with high affinity for both DNA and RNA (Kay, N., Bainbridge, T, Condit, C. and D'Costa, S., unpublished results; (Beaud et al., 1995; Kovacs & Moss, 1996; Nowakowski et al., 1978). H5 is differentially phosphorylated during infection implying that the interaction of H5 with different binding partners during infection is regulated by phosphorylation (Beaud et al., 1995; Beaud et al., 1994). Thus we envision the coupled processes of DNA replication and postreplicative gene transcription, and also morphogenesis, occuring on the H5 scaffold.

Previous experiments implicate H5 in DNA replication based solely on interactions between H5 and DNA replication proteins, specifically A20 and B1 (McCraith et al., 2000; Ishii & Moss, 2002). A20 is a DNA polymerase processivity factor that exists in a heterotrimeric replication complex along with the viral DNA polymerase (E9) and uracil DNA glycosylase (D4) (Stanitsa et al., 2006). Recently, Traktman and co-workers have observed that H5 co-purifies at near stoichiometric ratios with the overexpressed trimeric DNA replication complex (E9, A20, and D4), possibly via the interaction of H5 with A20 (P. Traktman, personal communication). B1 is a viral serine-threonine kinase required for DNA replication (Rempel & Traktman, 1992). Recently, it was determined that the primary if not the only role of the B1 kinase in viral DNA replication is to phosphorylate and thus inactivate BAF, a host protein involved in defending the cell against foreign DNA (Wiebe & Traktman, 2007). Interestingly, H5 is the only viral substrate for the B1 kinase (Beaud et al., 1994; Beaud et al., 1995; Beaud & Beaud, 2000). We hypothesize that viral DNA replication takes place on the H5 scaffold, mediated by the binding of H5 to nucleic acid and/or A20. We speculate further that the phosphorylation of H5 by the B1 kinase may be required for the interaction of H5 with B1, localizing B1 to the site of DNA replication and thereby enabling the phosphorylation of BAF at the site of viral DNA replication in the cytoplasm of the infected cell. Our model thus hypothesizes direct roles for H5 in DNA replication, consistent with the DNA negative phenotype of Dts57.

Published data have argued for a role for H5 in virtually every step of postreplicative transcription: initiation, elongation, and termination. Specifically, as detailed in the Introduction, H5 interacts with late gene transcription initiation factors (A2 and G8) and stimulates late gene transcription in vitro; H5 interacts with a postreplicative gene transcription elongation factor (G2) and can be mutated to confer resistance to the elongation enhancing drug IBT; H5 interacts with the postreplicative gene transcription termination factor (A18); and H5 is associated with an endoribonuclease activity implicated in postreplicative gene transcription termination (Dellis et al., 2004; Black et al., 1998; Cresawn & Condit, 2007; D'Costa et al., 2008; Kovacs & Moss, 1996; McCraith et al., 2000). Inactivation of H5 via temperature shift in a Dts57 infection results in accelerated decay of postreplicative transcripts relative to a Dts20 infection, consistent with a defect in transcription initiation. In the same temperature shift experiment, we also observed a decrease in intensity of the normal homogenous 1.5 kb late F17 transcript and the appearance of a faster migrating homogenous band. These findings suggest that the lesion in Dts57 affects either H5 mediated mRNA processing or transcription elongation. Extracts prepared from Dts57-infected cells using the temperature shift protocol were cleavage competent *in vitro* (data not shown); suggesting that the mRNA processing function of Dts57 is intact. Therefore, we hypothesize that Dts57 is defective in transcription elongation, resulting in synthesis of F17 transcripts that are shorter than normal.. This result is reminiscent of infections with mutants in other late gene elongation factors, J3and G2 (Latner et al., 2000), where discrete 3' truncated F17 transcripts were also observed. Thus the current study confirms that H5 mediates postreplicative transcription elongation and furthermore suggests that the elongation and mRNA processing functions of H5 are discrete. We suggest that the multiple roles of H5 in transcription are also mediated via

an H5 scaffold, which can bind both the DNA template, the RNA product, and several key factors involved in all steps of postreplicative gene transcription.

Our own results combined with previous studies by Traktman and co-workers show that H5 is involved in multiple steps of virus morphogenesis including membrane biogenesis, encapsidation of viroplasm to form IVs, and maturation of IVs to MVs. In tsH5–4 infections maintained at the non-permissive temperature from the outset of infection, viral membrane biogenesis is completely blocked in a fashion similar to infections with mutants in the F10 kinase, suggesting that H5 phosphorylation by F10 or modulation of F10 activity by H5 may play a critical role early in virus assembly (Traktman et al., 1995; Wang & Shuman, 1995; Demasi & Traktman, 2000; Condit et al., 2006; Mercer & Traktman, 2005). We show here that H5 is also required for viroplasm encapsidation to form normal IVs. Specifically, in the rifampicin release temperature shift protocol, tsH5–4 infection results in accumulation of membrane crescents, empty IVs and curdled virosomes, a phenotype similar to that observed for tsA30 and tsG7 infections (Mercer & Traktman, 2005). A30, G7 and F10 are components of a "seven protein complex" that is thought to be responsible for targeting viroplasm to membrane crescents and encapsidation of viroplasm into IV (Szajner et al., 2004). Mercer & Traktman (2005) have shown that both the G7 and A30 proteins are unstable in a tsH5–4 infection, and we have observed destabilization of G7 in tsH5–4 infections following rifampicin release and temperature shift. Thus the block to viroplasm encapsidation may result from destabilization of the seven protein complex. Traktman and co-workers have suggested that H5 is a matrix protein upon which the seven protein complex forms and within which F10 can phosphorylate the other seven protein complex components (Mercer & Traktman, 2005). Likewise, we suggest that both membrane formation and the early stages of virion assembly including encapsidation of viroplasm takes place on and is facilitated by the H5 scaffold. Lastly, in the rifampicin release temperature shift protocol, Dts57 infection results in a block in formation of MV from IV. Mutants in a wide variety of vaccinia gene functions exhibit a similar block to MV formation (Condit et al., 2006). H5 is normally encapsidated into the virion and is probably required for proper formation of core substructures.

Materials and methods

Eukaryotic cells and viruses

BSC40 cells, wild type vaccinia strains WR and IHDW, temperature-sensitive mutants tsH5–4, Dts57, and Dts20 and the conditions for their growth and infection have been described previously (Condit & Motyczka, 1981; Condit et al., 1983; Condit et al., 1996; Fuerst et al., 1986; Bayliss & Condit, 1995; Lackner et al., 2003; Demasi & Traktman, 2000; Dales et al., 1978). A permissive temperature of 31°C and restrictive temperature of 39.7°C was used for all virus infections. A multiplicity of infection of 10 (moi=10) was used for all experiments unless otherwise denoted.

Marker rescue

One-step marker rescue was accomplished as described previously (Kato et al., 2007; Kato et al., 2007). Briefly, BSC40 cells in 60 mm dishes were infected with Dts57 for 1 h at 39.7 °C at an moi determined empirically by terminal dilution. After the adsorption period, the inoculum was aspirated, replaced with 4 ml of OPTI-MEM and transfected with 1.5 μg of the appropriate PCR product using Lipofectamine reagent (Invitrogen). Cells were incubated at the non-permissive temperature for 4 days and subsequently stained with crystal violet.

DNA sequence analysis

Total DNA was isolated from infected BSC40 cells using the Qiagen DNeasy miniprep kit for the isolation of DNA from cells in culture according to the manufacturer's instructions. This

DNA and two primers that hybridize just outside the open reading frame were used to amplify the entire H5 gene. Sequencing was performed by the University of Florida ICBR DNA Sequencing Core Laboratory.

Analysis of DNA Replication

Analysis of viral DNA replication was carried out as described previously (Traktman & Boyle, 2004). Briefly, confluent 35 mm dishes of BSC40 cells were infected with wt and mutant viruses as indicated. At different times post-infection, cells were harvested, washed once with PBS, and resuspended in 450 μl of buffer containing 10X SSC (1.5 M NaCl; 150 mM Na-citrate) and 1M NH_4-acetate. Samples were subjected to three rounds of freeze-thawing and stored at −70°C. Twenty-five micro liters of each well-vortexed sample was then applied to a nylon transfer membrane (Nytran Supercharge, Schleicher & Schuell) in a vacuum manifold (Minifold II, Schleicher & Schuell). While still in the blotting apparatus, the DNA on the membrane was denatured with a solution of 0.5 M NaOH/ 1.5 M NaCl and neutralized with 10X SSC. Hybridization was carried out at 42 °C with a randomly ^{32}P labeled (DECAprime II kit (Ambion)) vaccinia *Hin*dIII E fragment in buffer containing 6× SSC; 0.5% SDS; 5× Denhardt's (0.1 % BSA (Sigma, Fraction V), 0.1 % PVP, 0.1 % Ficoll 400) and 100 μg/ml single stranded salmon sperm DNA). After hybridization, the blots were washed three times in 2X SSC at room temperature followed by two washes at 55 °C with 0.2X SSC/ 0.1 % SDS, and analyzed using a phosphor imager (Storm 860, GE Healthcare).

Analysis of RNA Synthesis

Monolayers of BSC40 cells were infected with wt and mutant virus as indicated. At various times post infection, total RNA was isolated using the RNeasy kit (Qiagen) following the manufacturer's directions. Two micrograms of each RNA sample in 10 μl was mixed with an equal volume of RNA sample loading buffer (Fermentas), denatured by incubating at 70 °C for 10 min and fractionated on a formaldehyde agarose gel (1.2% agarose, 2.2 M formaldehyde in 1× MOPS buffer (20 mM MOPS: 5 mM sodium acetate, 1 mM EDTA, pH 7.0)). The gels were blotted and hybridized as described previously (Shatzer et al., 2008).

Metabolic labeling of viral proteins

BSC40 cell monolayers were infected with the indicated viruses. At the various times indicated, the cells were washed with methionine-free DMEM (Sigma) and pulse labeled with the same medium containing 50 μCi ^{35}S-labeled cysteine and methionine (ProMix-GE Healthcare) for 30 min. at the appropriate temperature. After the pulse, the cells were lysed in SDS-sample buffer (50 mM Tris–HCl, pH 6.8; 1% SDS; 10% glycerol; 140 mM 2-mercaptoethanol; 0.1% bromophenol blue), and analyzed by SDS-PAGE and autoradiography.

Immunoblot assay

Samples were resolved by SDS-PAGE and transferred electrophoretically to nitrocellulose filters in transfer buffer (25 mM Tris, 192 mM glycine, 20% methanol). Filters were incubated with polyclonal antisera directed against H5 (1:20,000 −1:40,000) (Demasi & Traktman, 2000), G7 (1:1000) or A10 (1:2000). Anti-A10 rabbit serum was provided by Dr. Mariano Esteban (CNB-CSIC, Spain), anti-H5 and anti-G7 rabbit sera were provided by Dr. Paula Traktman (Wisconsin Medical School). The bound primary antibody was then detected using a horseradish peroxidase-conjugated secondary antibody (anti-rabbit; 1:5000) and chemiluminescent reagents (GE Healthcare).

Shift up analysis

For the temperature shift analysis, 35-mm (virus yield, protein synthesis, and DNA synthesis) or 60-mm dishes (RNA synthesis) of confluent BSC40 cells were infected with wt and mutant

viruses and incubated at 31°C or 39.7°C. At 9 hours post infection, several dishes from each set of virus infection were shifted up to 39.7°C. At various times post infection before and after the shift, cells were harvested for virus yield, DNA, RNA and protein synthesis as described elsewhere in Materials and Methods.

Rifampicin Release analysis

(i) Virus Yields. Monolayers of BSC40 cells (35 mm dishes) were infected with either IHDW, Dts57, or tsH5–4 in quadruplicate in the presence of 200 μg of rifampicin per ml at 31°C for 12 h. At this time, two out of four plates from each set of infections were shifted to 39.7°C, and the rest were maintained at 31°C. Furthermore, one plate from each set at each temperature was washed and resuspended in media lacking rifampicin, while the other dish was maintained in the presence of drug. The infection was then allowed to proceed for an additional 24 h, at which time, cells were harvested, and viral yield was determined by plaque assay. *(ii) Transmission EM.* A second set of three 60mm dishes containing confluent BSC40 cells were infected and processed as described above for virus yields. At 12 h p.i., one dish from each virus infection was processed for EM as described below. The remaining two dishes were washed twice and resuspended in media devoid of rifampicin. One dish was then incubated at 31°C and the other was shifted to 39.7°C for another 24h after infection. At 36 h p.i., cells were rinsed with cold 0.1M sodium cacodylate and fixed *in situ* with 1% glutaraldehyde in 0.1M sodium cacodylate containing 2mM $MgCl_2$, 1mM $CaCl_2$, and 0.25% NaCl, pH 7.24 at RT for 30–60 min before placing on ice. Electron microscopy was carried out at the University of Florida ICBR Electron Microscopy Core Laboratory. Briefly, fixed cells were buffer washed twice and scraped from the dish, centrifuged to pellet and encapsulated with 3% agarose type VII. Subsequent steps were processed with the aid of a Pelco BioWave laboratory microwave (Ted Pella, Redding, CA). Samples were washed in 0.1M sodium cacodylate, post fixed with 2% buffered osmium tetroxide, water washed and dehydrated in a graded ethanol series (25%, 50%, 75%, 95%, and 100%), and followed by 100% acetone. Dehydrated samples were infiltrated in graded acetone/Spurr epoxy resin and oven cured at 60°C. Cured resin blocks were trimmed, thin sectioned and collected on formvar copper slot grids, post-stained with 2% aq. uranyl acetate and Reynold's lead citrate. Sections were examined with a Hitachi H-7000 TEM (Hitachi High Technologies America, Inc. Schaumburg, IL) and digital images acquired with Veleta camera and iTEM software (Olympus Soft-Imaging Solutions Corp, Lakewood, CO). *(iii) Pulse-chase analysis*. A third set of five 35mm dishes of confluent BSC40 cells were infected in tandem with the infections carried out for virus yields. At 12 hours p.i., the cells were washed with methionine-free DMEM and pulsed with the same medium containing 50 μCi/dish ^{35}S-labeled cysteine and methionine (ProMix-GE Healthcare) for 30 min. at 31°C. Following the pulse, one of the five plates from each set of infections was washed once with PBS, and the cells were lysed in SDS-sample buffer. Two plates from each set were washed twice with DMEM containing rifampicin and 100ug/ml methionine (+ RIF) and resuspended in the same media. The other two plates in each set were washed twice with DMEM containing 100ug/ml methionine (− RIF) and resuspended in the same media. One plate from each subset (+ RIF and − RIF) was shifted to 39.7°C, and the other plate was maintained at 31°C. The infection was then allowed to proceed for an additional 24 h, at which time, cells were washed once with PBS, lysed in SDS-sample buffer, harvested and analyzed by SDS-PAGE and autoradiography.

Acknowledgments

We thank Dr. Paula Traktman for tsH5–4 and the anti-H5 and anti-G7 antibodies, Dr. Mariano Esteban for the anti-A10 antibody and Dr. Bernard Moss for help with rifampicin. This work was supported by grant RO1 18094 to RCC from the National Institutes of Health.

References

Bayliss CD, Condit RC. The vaccinia virus A18R gene product is a DNA-dependent ATPase. J.Biol.Chem 1995;270:1550–1556. [PubMed: 7829483]

Beaud G, Beaud R. Temperature-dependent phosphorylation state of the H5R protein synthesised at the early stage of infection in cells infected with vaccinia virus ts mutants of the B1R and F10L protein kinases. Intervirology 2000;43:67–70. [PubMed: 10773740]

Beaud G, Beaud R, Leader DP. Vaccinia virus gene H5R encodes a protein that is phosphorylated by the multisubstrate vaccinia virus B1R protein kinase. J.Virol 1995;69:1819–1826. [PubMed: 7853522]

Beaud G, Sharif A, Topa-Masse A, Leader DP. Ribosomal protein S2/Sa kinase purified from HeLa cells infected with vaccinia virus corresponds to the B1R protein kinase and phosphorylates in vitro the viral ssDNA-binding protein. J.Gen.Virol 1994;75(Pt 2):283–293. [PubMed: 8113749]

Black EP, Moussatche N, Condit RC. Characterization of the interactions among vaccinia virus transcription factors G2R, A18R, and H5R. Virology 1998;245:313–322. [PubMed: 9636370]

Condit RC, Lewis JI, Quinn M, Christen LM, Niles EG. Use of lysolecithin-permeabilized infected-cell extracts to investigate the in vitro biochemical phenotypes of poxvirus ts mutations altered in viral transcription activity. Virology 1996;218:169–180. [PubMed: 8615020]

Condit RC, Motyczka A. Isolation and preliminary characterization of temperature-sensitive mutants of vaccinia virus. Virology 1981;113:224–241. [PubMed: 7269240]

Condit RC, Motyczka A, Spizz G. Isolation, characterization, and physical mapping of temperature-sensitive mutants of vaccinia virus. Virology 1983;128:429–443. [PubMed: 6577746]

Condit RC, Moussatche N, Traktman P. In a nutshell: structure and assembly of the vaccinia virion. Adv.Virus Res 2006;66:31–124. [PubMed: 16877059]

Condit RC, Niles EG. Regulation of viral transcription elongation and termination during vaccinia virus infection. Biochim.Biophys.Acta 2002;1577:325–336. [PubMed: 12213661]

Cresawn SG, Condit RC. A targeted approach to identification of vaccinia virus postreplicative transcription elongation factors: genetic evidence for a role of the H5R gene in vaccinia transcription. Virology 2007;363:333–341. [PubMed: 17376501]

D'Costa SM, Antczak JB, Pickup DJ, Condit RC. Post-transcription cleavage generates the 3' end of F17R transcripts in vaccinia virus. Virology 2004;319:1–11. [PubMed: 14967483]

D'Costa SM, Bainbridge TW, Condit RC. Purification and properties of the vaccinia virus mRNA processing factor. J.Biol.Chem 2008;283:5267–5275. [PubMed: 18089571]

Dales S, Milovanovitch V, Pogo BG, Weintraub SB, Huima T, Wilton S, McFadden G. Biogenesis of vaccinia: isolation of conditional lethal mutants and electron microscopic characterization of their phenotypically expressed defects. Virology 1978;84:403–428. [PubMed: 622807]

Dellis S, Strickland KC, McCarry WJ, Patel A, Stocum E, Wright CF. Protein interactions among the vaccinia virus late transcription factors. Virology 2004;329:328–336. [PubMed: 15518812]

Demasi J, Traktman P. Clustered charge-to-alanine mutagenesis of the vaccinia virus H5 gene: isolation of a dominant, temperature-sensitive mutant with a profound defect in morphogenesis. J.Virol 2000;74:2393–2405. [PubMed: 10666270]

Fuerst TR, Niles EG, Studier FW, Moss B. Eukaryotic transient-expression system based on recombinant vaccinia virus that synthesizes bacteriophage T7 RNA polymerase. Proc.Natl.Acad.Sci.U.S.A 1986;83:8122–8126. [PubMed: 3095828]

Gordon J, Mohandas A, Wilton S, Dales S. A prominent antigenic surface polypeptide involved in the biogenesis and function of the vaccinia virus envelope. Virology 1991;181:671–686. [PubMed: 1707568]

Ishii K, Moss B. Role of vaccinia virus A20R protein in DNA replication: construction and characterization of temperature-sensitive mutants. J.Virol 2001;75:1656–1663. [PubMed: 11160663]

Ishii K, Moss B. Mapping interaction sites of the A20R protein component of the vaccinia virus DNA replication complex. Virology 2002;303:232–239. [PubMed: 12490386]

Kato SE, Condit RC, Moussatche N. The vaccinia virus E8R gene product is required for formation of transcriptionally active virions. Virology. 2007

Kato SE, Moussatche N, D'Costa SM, Bainbridge TW, Prins C, Strahl AL, Shatzer AN, Brinker AJ, Kay NE, Condit RC. Marker rescue mapping of the combined Condit/Dales collection of temperature-sensitive vaccinia virus mutants. Virology 2008;375:213–222. [PubMed: 18314155]

Kovacs GR, Moss B. The vaccinia virus H5R gene encodes late gene transcription factor 4: purification, cloning, and overexpression. J.Virol 1996;70:6796–6802. [PubMed: 8794318]

Lackner CA, D'Costa SM, Buck C, Condit RC. Complementation analysis of the dales collection of vaccinia virus temperature-sensitive mutants. Virology 2003;305:240–259. [PubMed: 12573570]

Latner DR, Xiang Y, Lewis JI, Condit J, Condit RC. The vaccinia virus bifunctional gene J3 (nucleoside-2'-O-)- methyltransferase and poly(A) polymerase stimulatory factor is implicated as a positive transcription elongation factor by two genetic approaches. Virology 2000;269:345–355. [PubMed: 10753713]

Luttge BG, Moyer RW. Suppressors of a host range mutation in the rabbitpox virus serpin SPI-1 map to proteins essential for viral DNA replication. J.Virol 2005;79:9168–9179. [PubMed: 15994811]

McCraith S, Holtzman T, Moss B, Fields S. Genome-wide analysis of vaccinia virus protein-protein interactions. Proc.Natl.Acad.Sci.U.S.A 2000;97:4879–4884. [PubMed: 10781095]

McDonald WF, Crozel-Goudot V, Traktman P. Transient expression of the vaccinia virus DNA polymerase is an intrinsic feature of the early phase of infection and is unlinked to DNA replication and late gene expression. J.Virol 1992;66:534–547. [PubMed: 1727498]

Mercer J, Traktman P. Genetic and cell biological characterization of the vaccinia virus A30 and G7 phosphoproteins. J.Virol 2005;79:7146–7161. [PubMed: 15890954]

Moss, B. Poxviridae: the viruses and their replication. In: Knipe, DM.; Howley, PM., editors. Fields Virology. Wolters, Kluwer-Lippincott, Williams and Wilkins; Philadelphia: 2007. p. 2906-2945.

Nowakowski M, Bauer W, Kates J. Characterization of a DNA-binding phosphoprotein from vaccinia virus replication complex. Virology 1978;86:217–225. [PubMed: 208247]

Punjabi A, Traktman P. Cell biological and functional characterization of the vaccinia virus F10 kinase: implications for the mechanism of virion morphogenesis. J.Virol 2005;79:2171–2190. [PubMed: 15681420]

Rempel RE, Traktman P. Vaccinia virus B1 kinase: phenotypic analysis of temperature-sensitive mutants and enzymatic characterization of recombinant proteins. J.Virol 1992;66:4413–4426. [PubMed: 1602551]

Romero P, Obradovic Z, Dunker AK. Natively disordered proteins: functions and predictions. Appl.Bioinformatics 2004;3:105–113. [PubMed: 15693736]

Rosel JL, Earl PL, Weir JP, Moss B. Conserved TAAATG sequence at the transcriptional and translational initiation sites of vaccinia virus late genes deduced by structural and functional analysis of the HindIII H genome fragment. J.Virol 1986;60:436–449. [PubMed: 3021979]

Shatzer AN, Kato SE, Condit RC. Phenotypic analysis of a temperature sensitive mutant in the large subunit of the vaccinia virus mRNA capping enzyme. Virology 2008;375:236–252. [PubMed: 18295814]

Sridhar P, Condit RC. Selection for temperature-sensitive mutations in specific vaccinia virus genes: isolation and characterization of a virus mutant which encodes a phosphonoacetic acid-resistant, temperature-sensitive DNA polymerase. Virology 1983;128:444–457. [PubMed: 6612992]

Stanitsa ES, Arps L, Traktman P. Vaccinia virus uracil DNA glycosylase interacts with the A20 protein to form a heterodimeric processivity factor for the viral DNA polymerase. J.Biol.Chem 2006;281:3439–3451. [PubMed: 16326701]

Szajner P, Jaffe H, Weisberg AS, Moss B. A complex of seven vaccinia virus proteins conserved in all chordopoxviruses is required for the association of membranes and viroplasm to form immature virions. Virology 2004;330:447–459. [PubMed: 15567438]

Szajner P, Weisberg AS, Lebowitz J, Heuser J, Moss B. External scaffold of spherical immature poxvirus particles is made of protein trimers, forming a honeycomb lattice. J.Cell Biol 2005;170:971–981. [PubMed: 16144903]

Traktman P, Boyle K. Methods for analysis of poxvirus DNA replication. Methods Mol.Biol 2004;269:169–186. [PubMed: 15114016]

Traktman P, Caligiuri A, Jesty SA, Liu K, Sankar U. Temperature-sensitive mutants with lesions in the vaccinia virus F10 kinase undergo arrest at the earliest stage of virion morphogenesis. J.Virol 1995;69:6581–6587. [PubMed: 7666563]

Unger B, Traktman P. Vaccinia virus morphogenesis: a13 phosphoprotein is required for assembly of mature virions. J.Virol 2004;78:8885–8901. [PubMed: 15280497]

Wang S, Shuman S. Vaccinia virus morphogenesis is blocked by temperature-sensitive mutations in the F10 gene, which encodes protein kinase 2. J.Virol 1995;69:6376–6388. [PubMed: 7666539]

Wiebe MS, Traktman P. Poxviral B1 kinase overcomes barrier to autointegration factor, a host defense against virus replication. Cell Host.Microbe 2007;1:187–197. [PubMed: 18005698]

Yao XD, Evans DH. High-frequency genetic recombination and reactivation of orthopoxviruses from DNA fragments transfected into leporipoxvirus-infected cells. J.Virol 2003;77:7281–7290. [PubMed: 12805426]

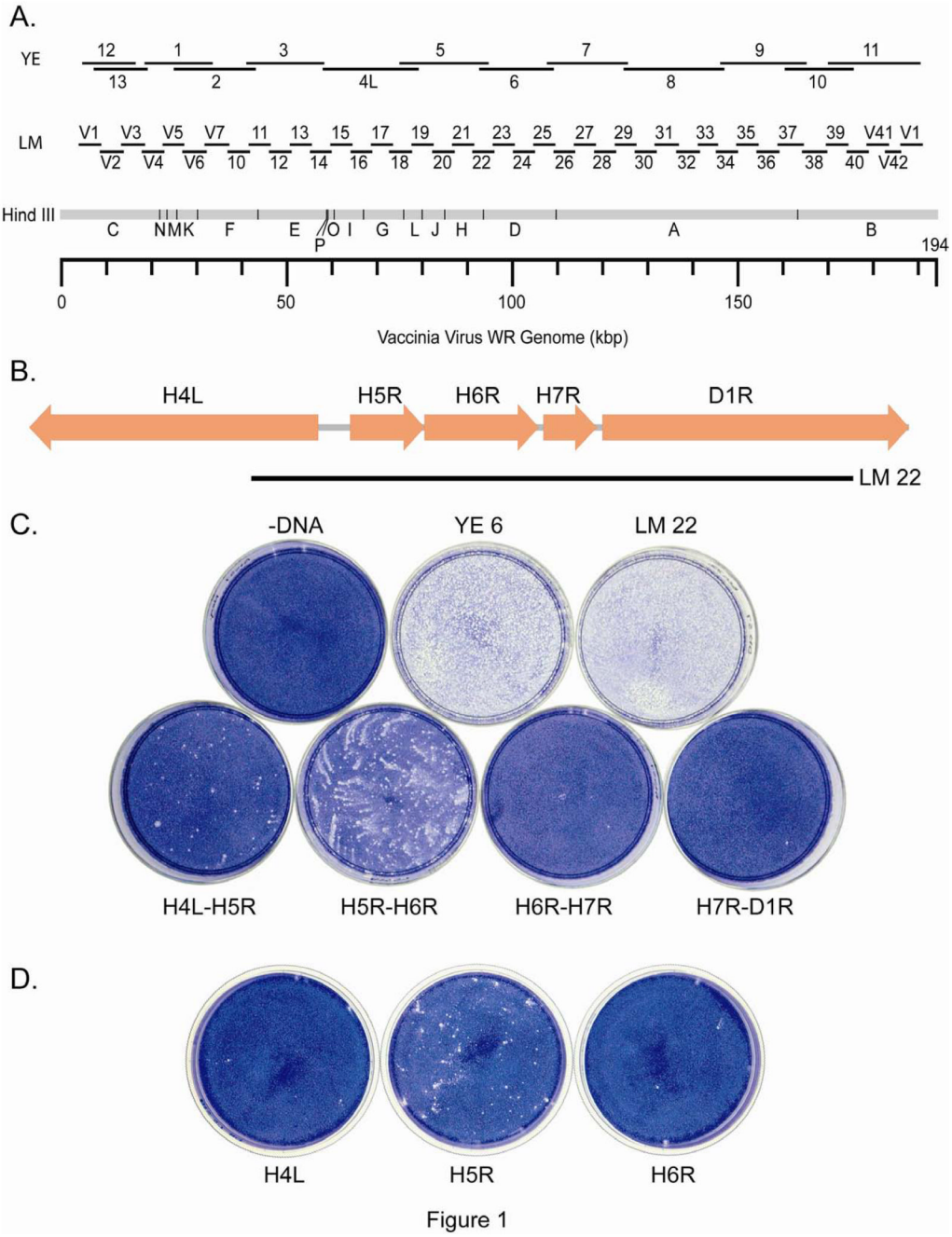

Fig. 1. Marker Rescue Mapping of Dts57

A) A HindIII map of the vaccinia genome showing the positions of the ~20-kb sized YE PCR fragments and the ~5-kb sized LM PCR fragments. B) A map of a portion of the HindIII H–D junction with the position of the genes (arrows) and LM22 PCR product indicated. C) Marker Rescue of Dts57. BSC40 cells were infected with Dts57, transfected with PCR fragments as indicated, incubated at 39.7°C for four days, and stained with crystal violet. D) Marker rescue of Dts57 with individual ORFS H4L, H5R, and H6R. Dishes were infected as described above and transfected with PCR products spanning the individual ORFs H4L, H5R, and H6R. A positive signal over background is seen only with H5R.

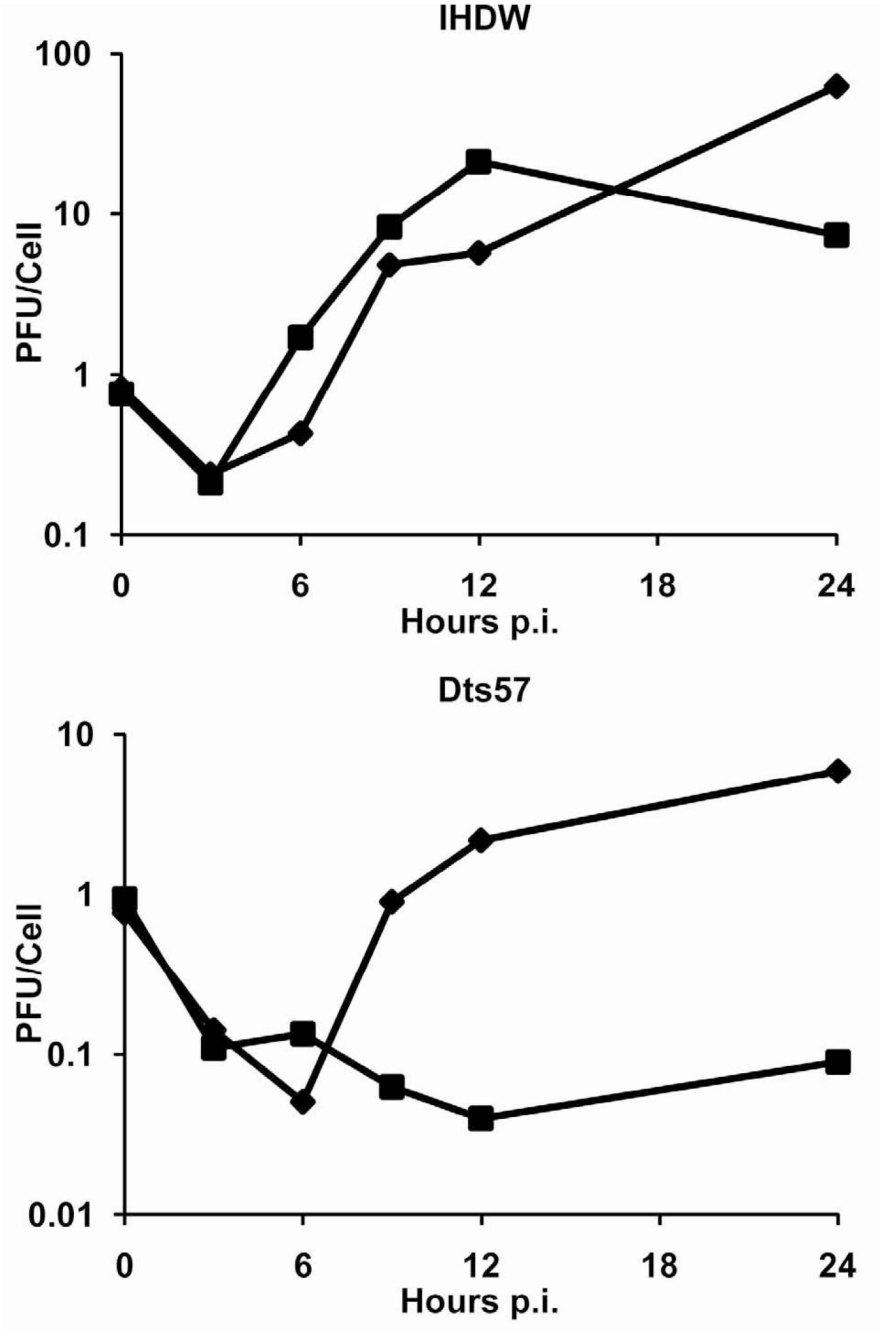

Fig. 2. One step growth curves for Dts57 and IHDW viruses

BSC40 cells were infected with the indicated virus at an moi of 10. Cells were harvested at the various times shown (x-axis) and virus titer determined by plaque assays at 31°C was plotted as pfu/cell (y-axis). A representative experiment is shown.

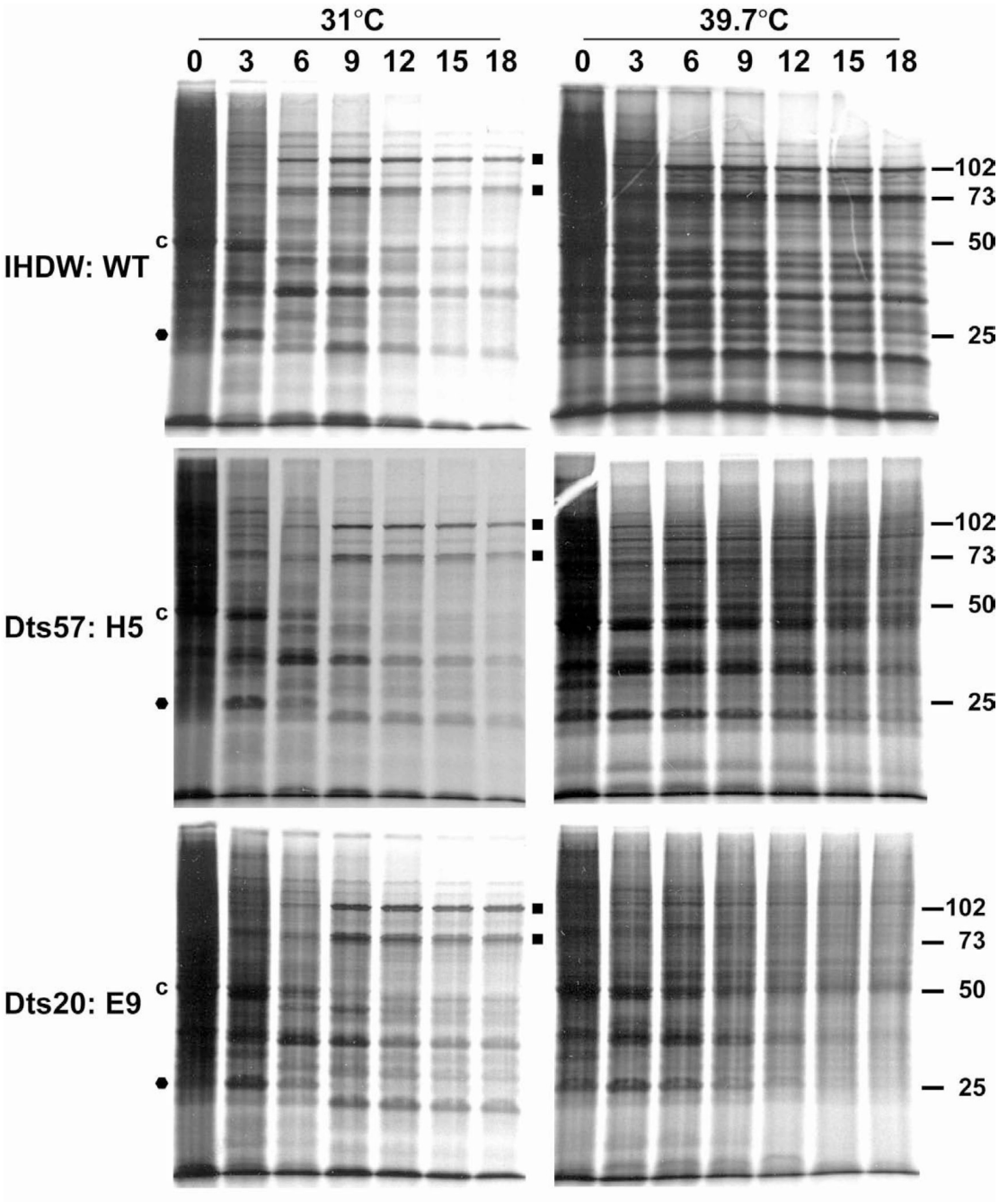

Fig. 3. Analyses of protein synthesis in Dts57, Dts20 and IHDW infections

Cells were infected with Dts57, IHDW, or Dts20 virus at an moi of 10 both at 31°C and at 39.7°C. At the various times indicated, infected cells were pulse labeled with ^{35}S-methionine for 30 min. at the appropriate temperature and harvested in SDS-sample buffer. Harvested cells were then fractionated by SDS-PAGE, fixed, stained with Coomassie blue, dried, and autoradiographed. Approximate molecular weight markers in kDa are indicated on the right, the times of harvest in hours and the temperature of infection are indicated at the top, and the identity of the virus is indicated on the left of the autoradiograms. Examples of the different classes of proteins are indicated as shown: c: host cell protein; ● early viral protein; ■: late viral protein.

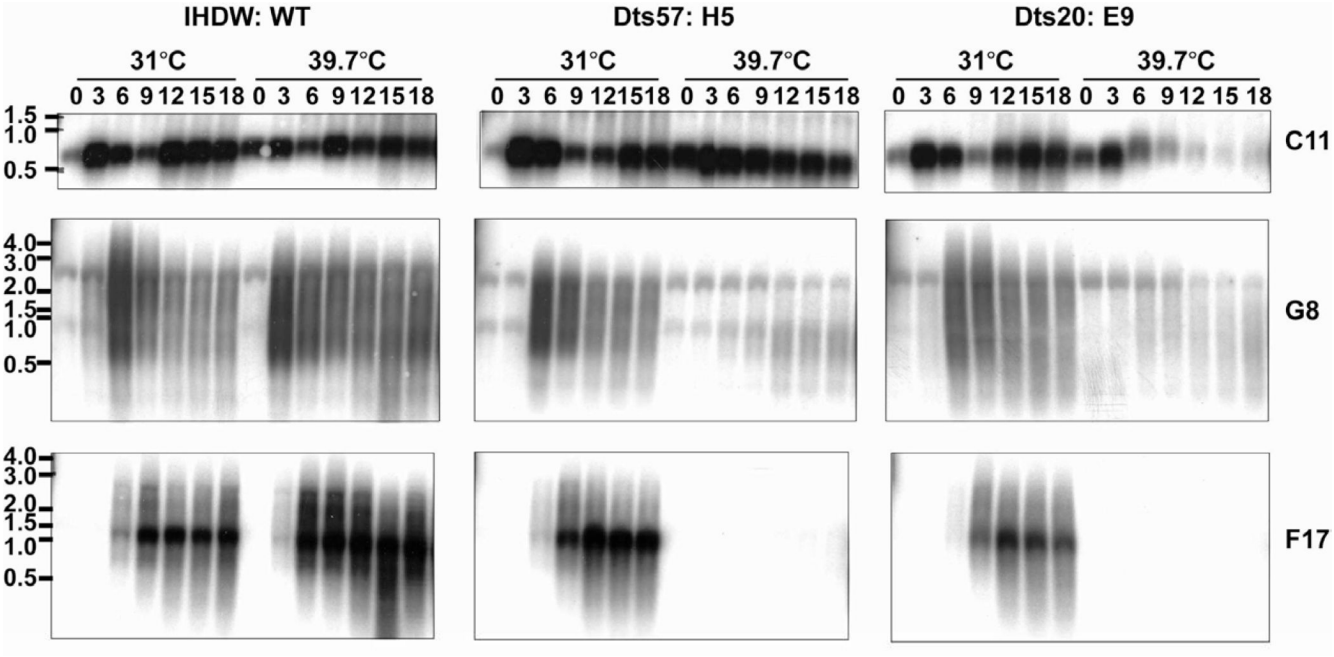

Fig. 4. Analysis of RNA synthesis in Dts57, IHDW, and Dts20 infections

Cells were infected with Dts57, IHDW, or Dts20 virus and incubated at 31°C or 39.7°C. Total RNA was extracted at the various times indicated, fractionated on formaldehyde-agarose gels and analyzed by northern blot analysis. Gene specific riboprobes representative of each class, early (C11), intermediate (G8) and late (F17) were used and are listed to the right of each autoradiogram. The virus with which the cells were infected, the temperature of incubation, and the time post-infection (in hours) are listed above the autoradiograms. Molecular weight markers in kb are listed to the left of the autoradiograms.

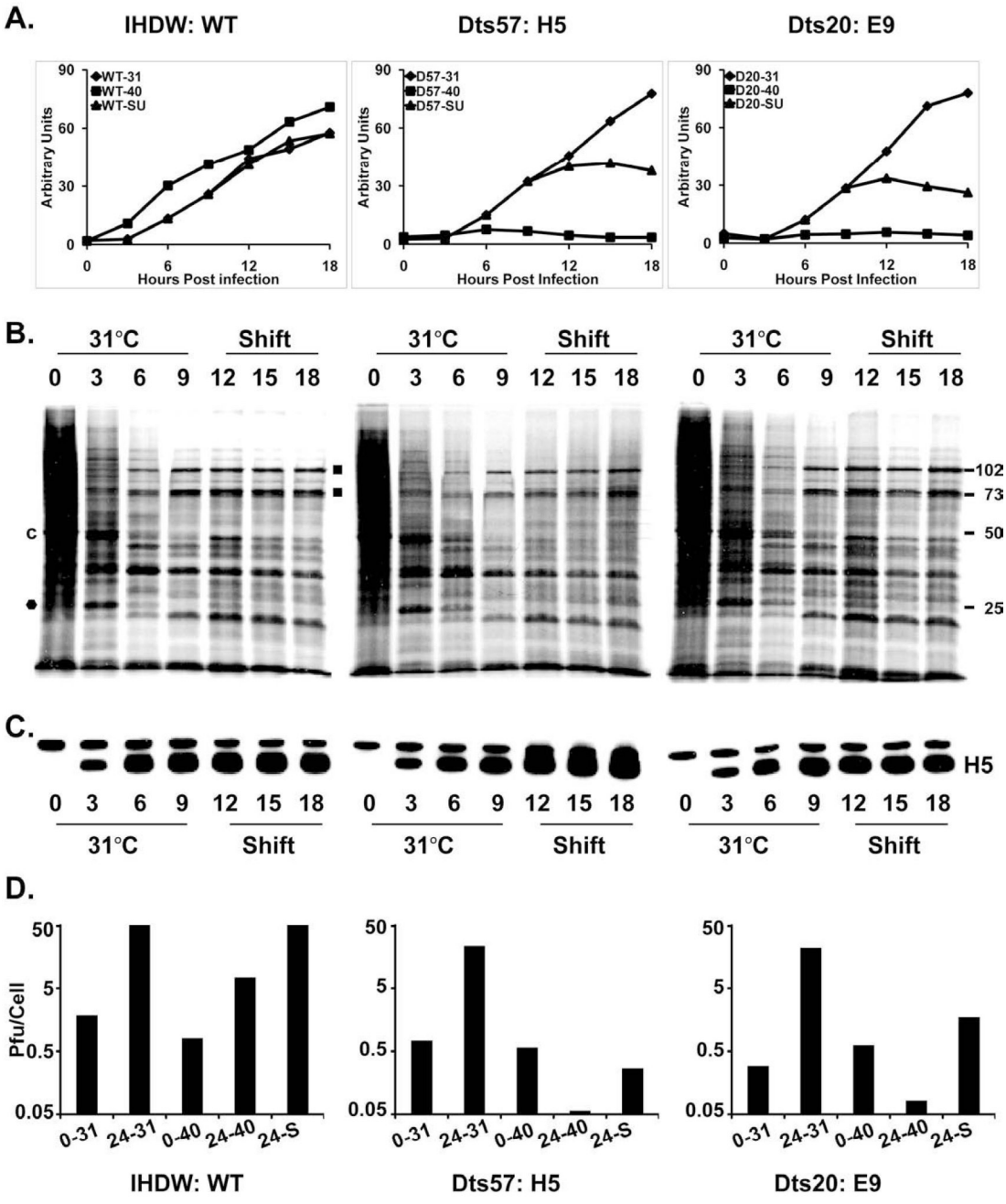

Fig. 5. Analysis of protein synthesis, H5 protein stability, DNA synthesis, and virus yield in Dts57, IHDW, and Dts20 infections in a temperature shift experiment

Cells were infected with Dts57, IHDW, or Dts20 virus at an moi of 10 and incubated at 31°C and 39.7°C (abbreviated as 40°C in the figure) as indicated. At 9 h p.i., a subset of the infected cells from 31°C was shifted up to 39.7°C for the remainder of the experiment. A) DNA synthesis in IHDW, Dts57, and Dts20 infections. At the various times post infection indicated (x-axis), infected cells were harvested and analyzed by slot blot hybridization with a radiolabeled vaccinia genome specific probe as described in Material and Methods. Samples were analyzed by blotting in triplicate and the data are represented as an average of these data points (y-axis). B) Protein synthesis in IHDW, Dts57, and Dts20 infections. At the various

times post infection, infected cells were pulsed with ^{35}S-methionine for 30 min at the appropriate temperature, harvested in Laemmli buffer and processed as described in Materials and Methods and Fig. 3. Approximate molecular weight markers in kDa are indicated on the right; the times of harvest in hours, the temperature of infection, and the identity of the virus are indicated at the top of the autoradiograms. Examples of the different classes of proteins are indicated as shown: c: host cell protein; ● early viral protein; ■ : late viral protein. C) Immunoblot analysis of H5 protein IHDW, Dts57, and Dts20 infections. Harvested protein samples from (B) were fractionated by SDS-PAGE, transferred to nitrocellulose membranes and probed with a polyclonal anti-H5 antibody. The faster migrating band is H5. The slower migrating band is a cellular protein present in mock infections. Note that H5 migrates anomalously at 35 kDa relative to its predicted MW of 22 kDa, as previously described (Gordon et al., 1991;Rosel et al., 1986;Beaud et al., 1995). The time of harvest in hours and the temperature of incubation are indicated at the bottom of the autoradiogram. D) Virus yield in IHDW, Dts57, and Dts20 infections. At the various times and temperatures indicated (x-axis), cells were harvested in culture media and analyzed by plaque assays at 31°C. A bar graph of virus yield in pfu/cell (y-axis) for the various conditions (x-axis) was plotted. The identity of the virus is indicated at the bottom of the graph.

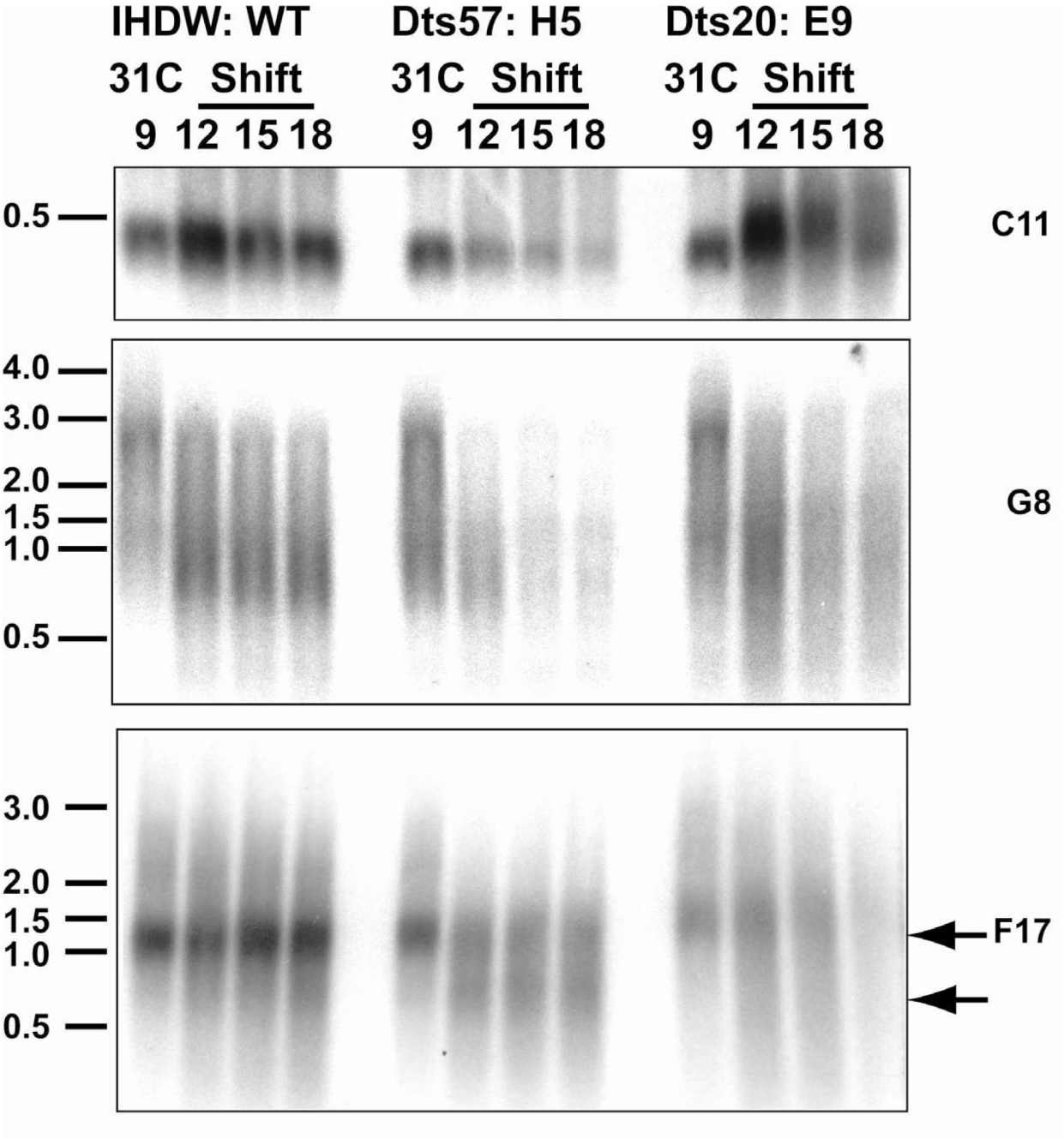

Fig. 6. Analysis of RNA synthesis in Dts57, IHDW, and Dts20 infections in a temperature shift experiment

Cells were infected with Dts57, IHDW, or Dts20 virus at an moi of 10 and incubated at 31°C and 39.7°C as indicated. At 9 h p.i., a subset of the infected cells from 31°C was shifted up to 40°C for the remainder of the experiment (shift). At the various times indicated, infected cells were harvested and analyzed by northern blot hybridization using riboprobes representative of each gene class: early (C11R), intermediate (G8R), and late (F17R). The time of harvest in hours, the temperature of incubation, and the identity of the infecting virus are indicated at the top of the autoradiogram. Molecular weight markers in kb are denoted on the left of the

autoradiogram and the identity of the riboprobes used are indicated on the right. The two arrows indicate the homogenous bands in the F17 autoradiogram.

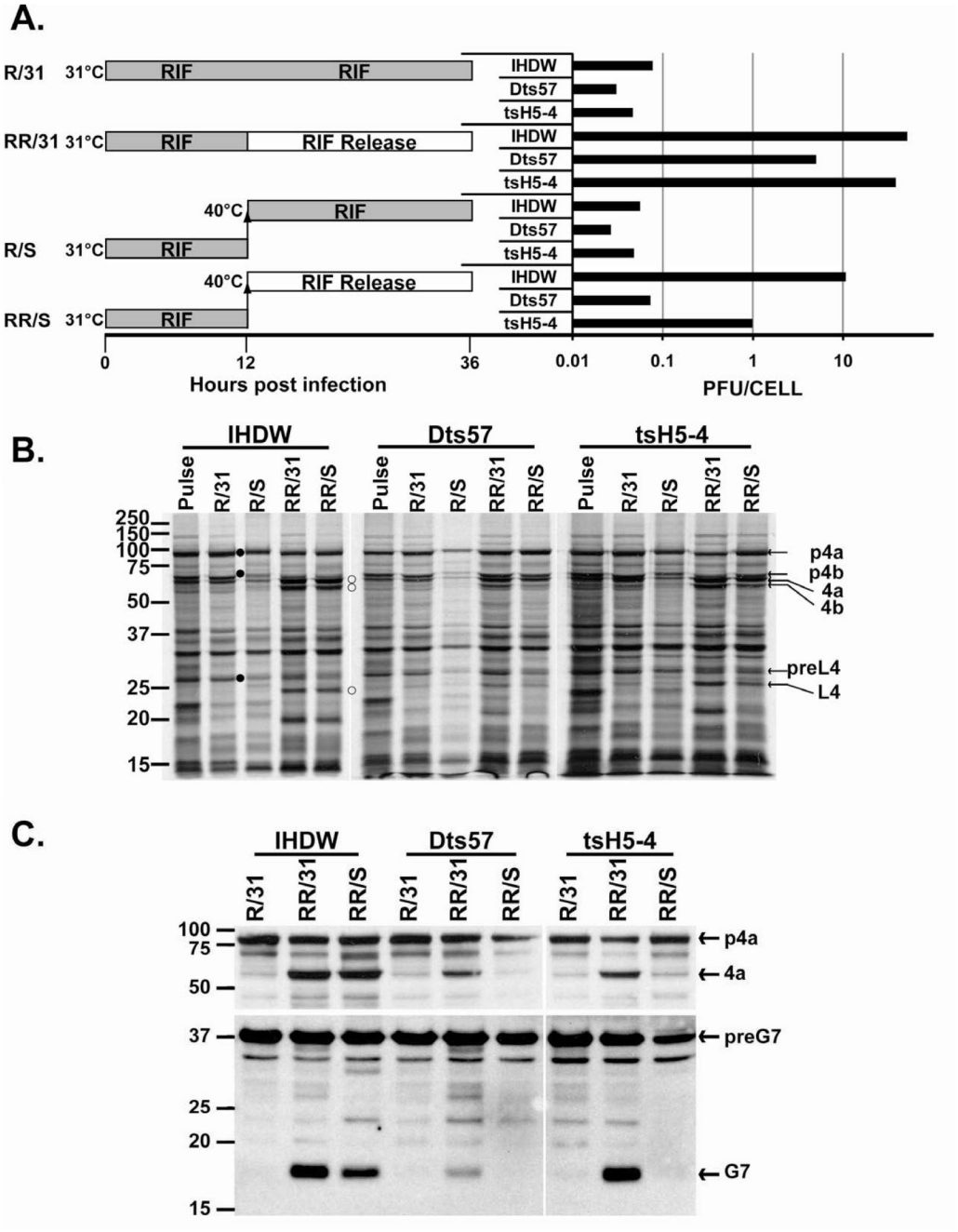

Fig. 7. Dts57 and tsH5–4 are defective in morphogenesis in a rifampicin release temperature shift protocol

BSC40 cultures were infected with wt (IHDW) and mutant (Dts57, tsH5–4) viruses in the presence of rifampicin at 31°C (permissive temperature). At 12 h p.i., cells were released from the rifampicin block and either left at 31°C (RR/31) or shifted up to 40°C (RR/S). Alternatively, the rifampicin block was maintained and the cells were left at 31°C (R/31) or shifted up to 40° C (R/S) until 36 h p.i. For protein synthesis and processing, tandem infections (as described above) were pulse labeled with ^{35}S-methionine at 12 h p.i., and then chased in cold medium +/− rifampicin at 31°C or shifted to 40°C for an additional 24 h. A) Schematic of the protocol with corresponding virus yield for each condition. B) Autoradiogram of pulse- and pulse-chase

samples. Closed circles indicate precursors and open circles indicate cleaved products. C) Immunoblot analyses for proteolytic cleavage of A10 and G7 proteins. The upper section of the blot was probed with anti-A10 antibody and the bottom section of the blot was probed with anti-G7 antibody.

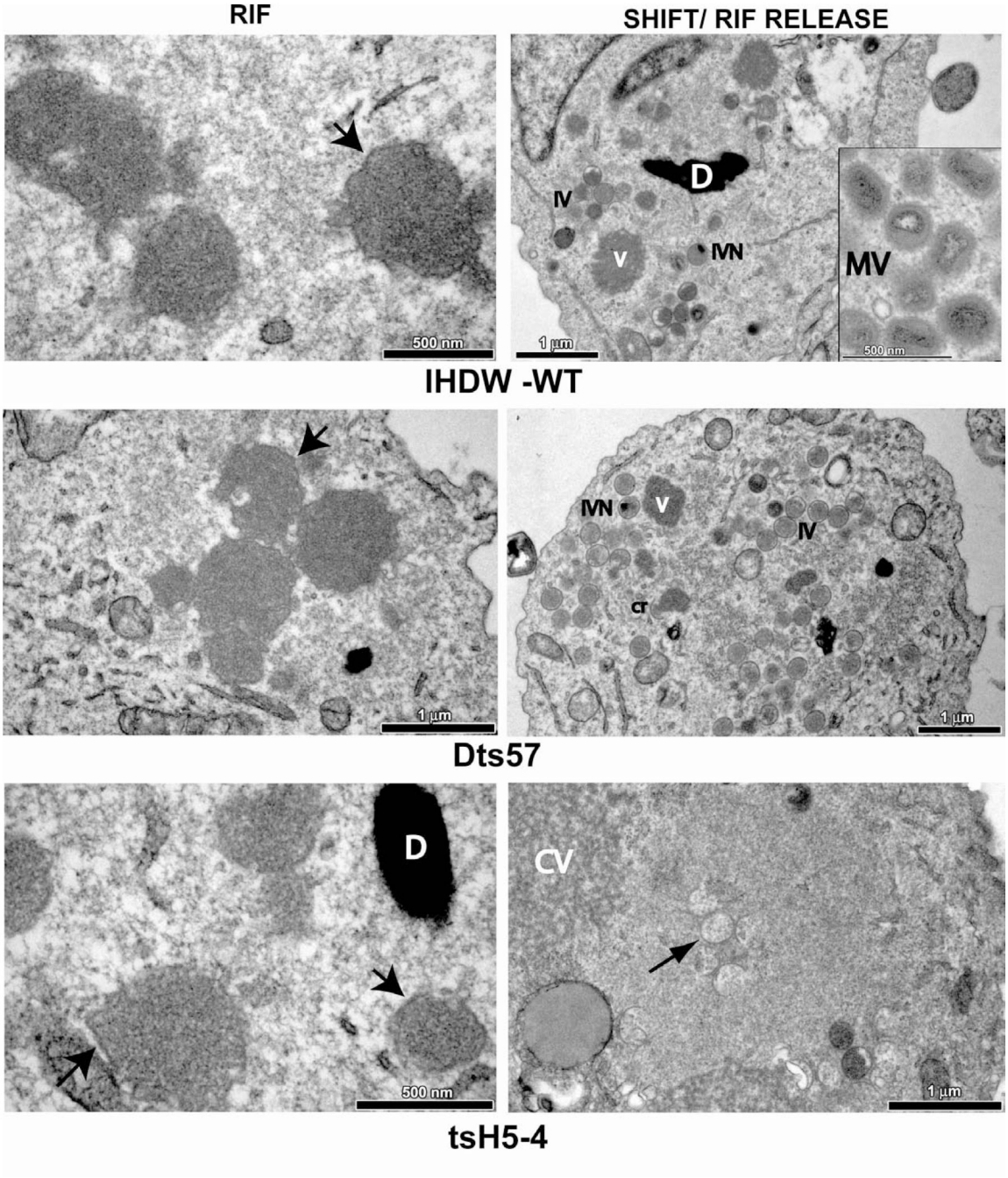

Fig. 8. H5 is required for IV formation and maturation of IV to MV

Cultures of BSC40 cells were infected with either wt (IHDW) or mutant (Dts57, tsH5–4) viruses at the 31°C in the presence of rifampicin. At 12 h p.i., rifampicin was washed out of the cells and shifted up to the non-permissive temperature (SHIFT/RIF RELEASE; right column) or cells were maintained in rifampicin at the permissive temperature (RIF; left column) for an additional 24 h. Characteristic rifampicin bodies are seen in the left column. Arrows indicate flaccid membranes surrounding the virosomes; D DNA crystalloids. Top plate; right column: Normal intermediates of morphogenesis are observed in wt infections: v virosomes; IV immature virions; MV mature virions. Middle plate; right column: Dts57 infections cannot progress beyond IV formation: v virosomes; IV immature virions. Bottom plate; right column:

tsH5-4 infections are arrested at IV formation. Clearing of the cytoplasm with empty IVs and crescents (arrow) were observed with curdled virosomes (CV) and few dense IVs in the periphery of the clearing.